THE EMERGENT STRUCTURE OF THE DROSOPHILA WING
A Dynamic Model Generator

Alberto Silletti

Department of Information Engineering, University of Padova, Via Gradenigo 6A, Padova, Italy
silletti@dei.unipd.it

Angelo Cenedese

Department of Engineering and Management, University of Padova, Vicenza, Italy
angelo.cenedese@unipd.it

Alessandro Abate

Department of Aeronautics and Astronautics, Stanford University, Stanford (CA), U.S.A.
aabate@stanford.edu

Abstract: Drosophila melanogaster is a model organism in genetics thanks to the compactness of its genome and its relative simplicity. Recently, certain developmental patterns in Drosophila have been studied by mathematical models, with the aim of gaining deeper and quantitative insight into the morphogenesis of this insect. There is a need for accurate dynamical of the epithelial cell structure and organization within the fly wing, to further the understanding of a phenomenon known as planar cell polarity. The present study tackles the problem of retrieving such a salient structure using classical tools of dynamical system theory embedded with network and graph concepts. On the one hand the goal is to provide a visual detection and representation of the cell packaging that is accurate and fine. Particular care is also put in obtaining a model of this structure, whose main features are the compactness and simplicity.

1 INTRODUCTION

Drosophila melanogaster is a *model organism* in developmental biology. Scientific interest in this organism can be traced back to some early work in genetics, and more recently the understanding of this insect has progressed with the investigation of its early development and the sequencing of its relatively compact genome. The relative simplicity of its morphogenesis allows to edulcorate the study of its development from many complications. Many human disease genes can be investigated and understood through analogues in the fruit fly. An important issue for the fly morphogenesis is the study of the polarization of cells on its wing. A mechanistic approach to study this phenomenon has led to some understanding of the underlying structures and regulatory proteins in the epithelial cells of the fly wing (Amonlirdviman et al., 2005). The dynamical model hinges on the assumption that the cell are regularly packed in a honeycomb structure throughout the wing. In order to understand how to extend these models, it makes sense to infer the structure and motion of the network of epithelial cells by looking at the phenotype of the fly wing with movies taken in the laboratory. This suggests to split the approach into two sequential steps:

1. first, given a single frame of the fly wing, build a network that closely represents the cell packing;

2. then, given a movie (a sequence of frames) of the fly wing, correlate the networks generated by considering single frames into a time-dependent dynamical model.

In this article we report on the former point, while the extension of the study is currently under investigation.

The goal of this study is twofold. On the one hand we try to detect the structure on the drosophila wing and provide a visual representation. On the other hand, we produce a model of the same structure, whose main features are the compactness and the simplicity.
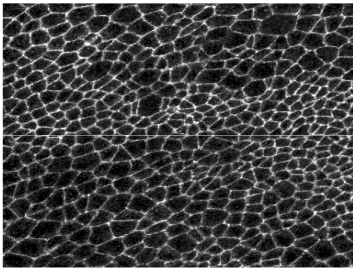
Figure 1: Drosophila wing epithelial cells.

The following approach is thus developed both to retrieve the network structure as a fine representation and to abstract the information related to the structure into a manageable model. This is obtained by exploring the visual data through a dynamic random walk model, whose motion state summarizes the useful information and allows the full detailed reconstruction of the network. To give a pictorial idea, the image frame is considered as a landscape where clear paths have to be discerned from darker areas. The agent performing the detection advances by scanning the neighborhood of his current position in search for explorable paths. When a bifurcation occurs the agent generates one or more siblings that start to move independently, until the whole frame has been explored.

The remainder of the paper is organized as follows. After an overview of the state of the art in structure detection (Sec. 2) and a description of the procedure for image preprocessing (Sec. 3), the adopted model is introduced in Sec. 4 and the algorithm explained in Sec. 5. Then, the static analysis of the image frame is discussed in Sec. 6 and, finally, in Sec. 7 some conclusions are drawn and insight on future developments is given.

2 THE STATE OF THE ART

The recognition of structures in digital images is a crucial task in many automated algorithms used in computer vision. For the task of edge detection, several approaches based on derivatives have been proposed, among which the seminal studies by Sobel (Sobel, 1968) and Prewitt (Prewitt, 1970) and Canny (Canny, 1986).

These approaches though are prone to failure, since they do not incorporate any prior knowledge of the object, nor do they include any geometrical model. This can yield very fragmented edges and many false classifications. They also do not return any compact and light representation of the recognized pattern. Such algorithms are good to *represents* patterns, but not to *model* them. The Canny edge detector out-

puts a bitmap map, where each pixel is classified as belonging to a border or not. Indeed, no *structure* is returned, and no compact model is given to the user. If there is a need for computing metrics or for analytically following a path around the edges, this approach appears to be unsatisfactory.

Active Contours (Blake and Isard, 1998) based approaches give better results, thanks to the elastic model structure they incorporate. Active Contours and Deformable Models (McInerney and Terzopoulos, 1996) generally perform well in shape recognition. Still, they are very sensitive to noise, they need a good initialization point to converge, and they require hard-tuning of the parameters to make things really work.

For thin linear structures such as vessels, marble veins, roads on terrain, better results can be achieved using a model of the motion over the image, which attempts to follow the structure of interest (Grisan et al., 2003). This approaches is promising and achieves near optimal results. A random motion paradigm can also be used also for image segmentation (Harel and Koren, 2001) and image enhancement (Smolka and Wojciechowski, 2001).

3 IMAGE PREPROCESSING

The images retrieved from biological experiments are particularly noisy and exhibit poor contrast, with non-uniform background illumination, resulting in structure boundaries not sufficiently sharp to be segmented. The preprocessing stage presented consists of four sequential steps (see Fig.2):

1. the image is filtered with a low-pass gaussian filter to soften high frequency noise;

2. an erosion filter suppresses the isolated bright pixels and decreases the intensity of cell edges, while retaining all the significant information;

3. an histogram stretch allows to partially recover the color dynamic range;

4. an image intensity power enhances the contrast.

4 THE DYNAMICAL MODELS

In this section the principle underlying the algorithm is briefly described. To retrieve the salient structure in the video sequence and to circumvent issues related to disconnected edges and false recognition (such as those mentioned in Sec. 2), the edge detection problem is re-interpreted as the problem of exploring a digital frame in search of the connected tracks. Each
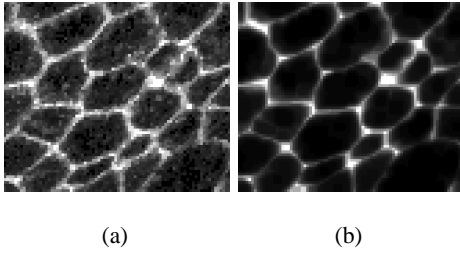
Figure 2: Image preprocessing: original (a) and preprocessed (b) frames.

digital picture is viewed as a *landscape* that has to be explored and where bright pixels–belonging to the edges of the cells–are thought of as *roads*, and dark pixels–the interior of the cells–as unexplored locations.

The idea behind the algorithm for robust and fast reconstruction of the interesting structure is based on a two level model, referred to respectively as an *explorer agent system* and as a *network agent system*. The *explorer agent* will retrieve the structure and provide a visual representation as fine as possible, while then *network agent* will abstract a compact model.

An explorer agent system $\mathcal{A}$ is defined according to a walk model, whose state equation is:

$$\mathbf{p}(t+1) = \mathbf{p}(t) + g(\theta(t)), \qquad (1)$$

$$\mathbf{p}(t) = \left[\begin{array}{c} x(t) \\ y(t) \end{array} \right] \in \mathbb{L},$$

$\mathbf{p}(t)$ is the current point position on the discrete domain $\mathbb{L} \subset \mathbb{Z}^2$ of the image frame and $g(\cdot)$ is a motion function. In the specific case,

$$g(\theta(t)) = k \left[\begin{array}{c} sin(\theta(t)) \\ cos(\theta(t)) \end{array} \right],$$

k being a design constant and $\theta(t)$ being the heading direction, which assumes the role of the input to the agent system.

The observation equation is the following:

$$\mathbf{y}(t) = \left[\begin{array}{c} x(t) \\ y(t) \\ \theta(t) \end{array} \right] = \left[\begin{array}{cc} 1 & 0 \\ 0 & 1 \\ 0 & 0 \end{array} \right] \mathbf{p}(t) + \left[\begin{array}{c} 0 \\ 0 \\ 1 \end{array} \right] \theta(t).$$

Several instances of the explorer agent, $\{\mathcal{A}_i, i = 1, \ldots, N_{\mathcal{A}}\}$, are concurrently present in the field of vision, and each generates at any time one or more directions viable to advance the exploration. Precisely, for each $\mathcal{A}_i$ the set of possible directions $\{\theta_{i,j}, j = 1, \ldots, m_i\}$, originating new agents, are collected in the vector $\Theta_i \in \mathbb{R}^{m_i}$.

Globally, the observations $\mathbf{y}(t)$ of all the explorer agents $\mathcal{A}_i$ yield a graph model $\mathcal{G} = (\mathcal{N}, \mathcal{E})$ (being $\mathcal{N}$ and $\mathcal{E}$ nodes and edges, respectively), where each

node $n_i \in \mathcal{N}$ is characterized by the state $\{x, y, \Theta\}$ of the locations visited by one of the $\mathcal{A}_i$, and the edges keep track of the path traveled by each agent (see Fig. 3). This graph provides a good *representation* of the retrieved structure, in the sense suggested in Section 2.
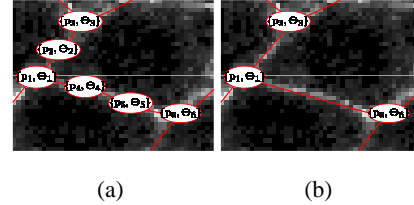

Figure 3: *Representation* and *Model* graphs $\mathcal{G}$ (a) $\mathcal{G}_r$ (b).

For modeling purposes, the goal is to obtaining compact-size models, flexible and agile. In this respect, only the subset $\mathcal{N}_r$ of the nodes associated to non-scalar Θ (and the correspondent edges $\mathcal{E}_r$) are interesting in the description, that is:

$$\mathcal{G}_r = (\mathcal{N}_r, \mathcal{E}_r) \; \mathcal{N}_r \subset \mathcal{N} \, s.t. \dim(\Theta(n_i)) > 1 \forall n_1 \in \mathcal{N}_r,$$

where $\dim(\Theta(n_i))$ indicates the cardinality of vector Θ for node n_i. If the border effects are neglected, the resulting graph $\mathcal{G}_r$ is a 3-connected graph, in which the minimum vertex degree is $d = 3$.

4.1 Brightness Function

We now explain how to choose the input direction $\theta(t)$. With reference to the pictorial interpretation, the aim is to explore the surroundings of the current position and to move from a bright location to another bright location. Thus a good direction of movement will be a direction that maximizes some sort of *brightness* function. Local brightness information is obtained by means of a function $L(\theta) : [0, 2\pi) \to \mathbb{R}$ built with the specific purpose of finding good directions of exploration. Sectors centered on the current position $\mathbf{p}$ are spanned, and for each sector the average brightness is computed. Formally, given a sector Ω_i, with any generic shape, we have

$$L(\theta_i) = \frac{\int_{\Omega_i} I(\omega) d\omega}{\int_{\Omega_i} d\omega} \qquad (2)$$

A natural choice for Ω_i is circular sector. Sectors of different shapes can also be built: For the problem of interest rectangular sectors also result to be quite effective.

After smoothing and thresholding the function, local maxima are collected as putative direction for the motion. Let $\Theta = \{\theta_1, \theta_2, \cdot, \theta_n\} = \arg \max_\theta L(\theta)$.
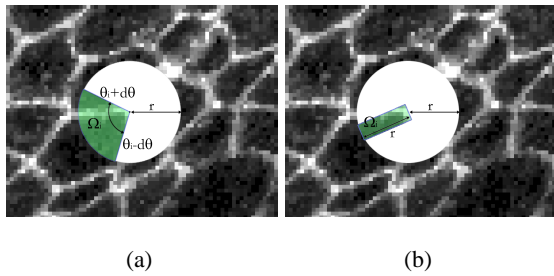
(a)   (b)

Figure 4: A brightness function built on circular sectors is a natural choice, since it mimics the field of view of human beings (a). Other shapes for sectors are also possible, depending on the problem under study: in the specific case, a rectangular shape efficiently serves the purpose (b).
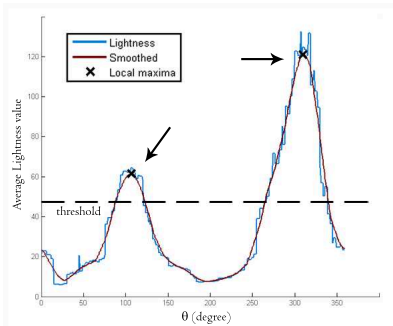

Figure 5: Local maxima of the brightness function identify candidate directions of expansion.

5 THE ALGORITHM

The initialization of the algorithm consists of a single agent $\mathcal{A}_0$ exploring the frame. At each motion step, the arguments of local maxima of L provide the set Θ of candidate directions. A Priority Queue Q is defined by inserting either the agent $\mathcal{A}_0$ with its heading direction and its corresponding brightness value or, when multiple directions m_i are possible, instances of $\mathcal{A}_0$ along with the direction $\theta_i \in \Theta$. Each of these agents is then put in motion according to Eq. 1.

The priority queue is sorted according to the brightness function associated with the current location of each agent. At each iteration step, the agent $\mathcal{A}_i$ with the highest brightness value is extracted and the exploration process is iterated. The role of the priority queue is thus to keep in memory the front of the expansion, and at the same time, to give the best possible expansion point, in the sense that the first agent in the queue will move to the best (i.e. brightest) area of the image.

By doing so, the algorithm is building a graph $\mathcal{G}$, where each node is the location $\mathbf{p_i}$ of an agent $\mathcal{A}_i$ extracted from the priority queue, and each arc joins a node and its nearest ancestor. Interpreting the under-

lying structure of the walk as a graph allows to resort to graph theory (Cormen et al., 1990) to refine the procedure.

5.1 Graph Structure Refinement

Small loops have to be avoided. Small loops are frequent in extensive bright areas of the image, where the brightness function $L(\theta)$ is not prone to differentiate between redundant directions. In these situations, a direction is as likely as any other, and the choice is driven mainly by randomness. When this happens we get $|\Theta| >> 1$ and $\theta_i \approx \theta_{i+1} \; \forall \; \theta_i \; \in \; \Theta$. In other words, all the values of $\theta_i \in \Theta$ are very similar and these directions spans uniformly the surrounding environment, so there is no particular reason to pick one direction over another.

In order to avoid this, after extracting a point from the queue, it is tested for loop creation in the graph. Large loops are accepted because they correspond to an actual closed path (for instance the perimeter of a cell), while small loops are disregarded.

A joining procedure is then required to fill small gaps: If two valid agents $\mathcal{A}_i$ and $\mathcal{A}_j$ end up close to each other, $|\{x,y\}_i - \{x,y\}_j| < \varepsilon$, they are joined together.

The algorithm also marks as *boundary nodes* those nodes close to the boundary of the digital image: The expansion process ends there (see Fig. 6(b)) and the agent $\mathcal{A}_i$ stops.

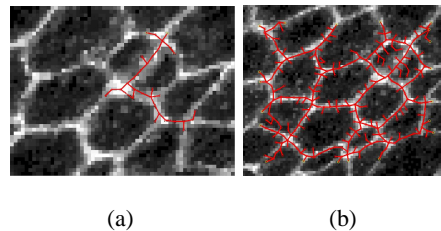(a)   (b)

Figure 6: (a) Small loops are frequent and are mainly due to the locality feature of the brightness function. (b) Raw results before postprocessing: many small spurious branches span over the interior of the cells.

The expansion process could create dead-branches, characterized by extremal non-border nodes of degree 1. A polished graph is obtained iteratively removing all such nodes and related edge. occurs.

The *network agent system* reconstruct the final geometric model of the cells considering only nodes with degree $d > 2$ and border nodes, considered the *corner* of the cells. The new graph $\mathcal{G}_r$ consists of such corners and new edges created between them if in the original graph there was a *straight* path (a path con-

necting them not passing through any other corner). The model reconstruction thus prunes a lot of nodes and edges and ends up with a light, compact representation of the cellular structure, achieving the second goal of this paper.

6 STATIC ANALYSIS

Preliminary results show a good accuracy in retrieving the salient structure on the fly wing and robustness in the detection procedure, for all the tested sequences. In Fig. 7 results obtained with the proposed technique are shown. The two cases are indicative of the critical issues that need to be faced, such as non-uniform illumination, different radii of the cells, noisy images.
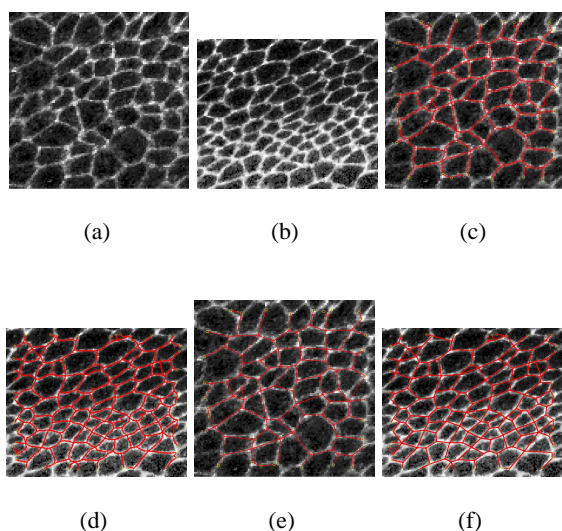

Figure 7: Example frames: a) -b) original; c) -d) representation $\mathcal{G}$; e) -f) model $\mathcal{G}_r$.

It is interesting to show the dynamic evolution of the exploration of the frame. A video showing the full procedure can be found at http://www.youtube.com/watch?v=I2HfKTCEd6w.

7 CONCLUSIONS AND FUTURE DEVELOPMENTS

In this work a procedure to detect salient lattice features from biological images has been developed, with the twofold purpose of representation and modeling. So far, the problem of the static reconstruction from single frames has been addressed, with encouraging results both for the accuracy of the details and for the robustness of the technique.

As a first step towards the dynamic reconstruction and tracking will be obtained by simply applying several times, once per frame, the static analysis (Sec. 6). A video obtained through this approach is available at http://it.youtube.com/watch?v=WxWjZSvuoh4. A fully dynamic tracking is still under study, and more refined dedicated approaches will be developed by exploiting temporal and local coherence.

REFERENCES

Amonlirdviman, K., Khare, N., Tree, D., Chen, W., Axelrod, J., and Tomlin, C. (2005). Mathematical modeling of planar cell polarity to understand domineering nonautonomy. *Science*, 307:423–426.

Blake, A. and Isard, M. (1998). *Active Contours*. Springer-Verlag, New York, USA.

Canny, J. (1986). A computational approach to edge detection. *IEEE Trans Patter Analysis and Machine Intelligence*, 8(6):679–698.

Cormen, T., Leiserson, C., and Rivest, R. (1990). *Introduction to Algorithms*. The MIT Press and McGraw-Hill.

Grisan, E., Foracchia, M., and Ruggeri, A. (2003). A novel method for the automatic grading of retinal vessel tortuosity. *Engineering In Medicine and Biology Society. Proc. of the 25th Annual International Conference of the IEEE*, 1(1):866–869.

Harel, D. and Koren, Y. (2001). On clustering using random walks. *Proc. of the 21st Conference on Foundation of Software Technology and Theoretical Computer Science*, 2245(1):18–41.

McInerney, T. and Terzopoulos, D. (1996). Deformable models in medical image analysis: a survey. *Medical Image Analysis*, 1(2):91–108.

Prewitt, J. (1970). *Object enhancement and extraction in Picture Processing and Psychopictorics*. Academic Press, New York.

Smolka, B. and Wojciechowski, K. (2001). Random walk approach to image enhancement. *Signal Processing*, 81:465–482.

Sobel, I. (1968). A 3x3 isotropic gradient operator for image processing. Unpublished, presented in a talk a the Stanford Articifial Project.